RESEARCH ARTICLE

Biofactors WILEY

The influence of redox modulation on hypoxic endothelial cell metabolic and proteomic profiles through a small thiol-based compound tuning glutathione and thioredoxin systems

Michela Bruschi[1] | Federica Biancucci[1] | Sofia Masini[1] |
Francesco Piacente[2] | Daniela Ligi[1] | Francesca Bartoccini[1] |
Antonella Antonelli[1] | Ferdinando Mannello[1] | Santina Bruzzone[2,3] |
Michele Menotta[1] | Alessandra Fraternale[1] | Mauro Magnani[1]

[1]Department of Biomolecular Sciences, University of Urbino Carlo Bo, Urbino, PU, Italy

[2]Department of Experimental Medicine, Section of Biochemistry, and CEBR, University of Genoa, Genoa, GE, Italy

[3]IRCCS, Ospedale Policlinico San Martino, Genoa, GE, Italy

Correspondence
Michela Bruschi, Department of Biomolecular Sciences, University of Urbino Carlo Bo, 61029 Urbino, PU, Italy.
Email: michela.bruschi@uniurb.it

Abstract

Reduction in oxygen levels is a key feature in the physiology of the bone marrow (BM) niche where hematopoiesis occurs. The BM niche is a highly vascularized tissue and endothelial cells (ECs) support and regulate blood cell formation from hematopoietic stem cells (HSCs). While in vivo studies are limited, ECs when cultured in vitro at low O_2 (<5%), fail to support functional HSC maintenance due to oxidative environment. Therefore, changes in EC redox status induced by antioxidant molecules may lead to alterations in the cellular response to hypoxia likely favoring HSC self-renewal. To evaluate the impact of redox regulation, HUVEC, exposed for 1, 6, and 24 h to 3% O_2 were treated with N-(N-acetyl-l-cysteinyl)-S-acetylcysteamine (I-152). Metabolomic analyses revealed that I-152 increased glutathione levels and influenced the metabolic profiles interconnected with the glutathione system and the redox couples NAD(P)+/NAD(P)H. mRNA analysis showed a lowered gene expression of *HIF-1α* and *VEGF* following I-152 treatment whereas *TRX1* and *2* were stimulated. Accordingly, the proteomic study revealed the redox-dependent upregulation of thioredoxin and peroxiredoxins that, together with the glutathione system, are the main regulators of intracellular ROS. Indeed, a time-dependent ROS production under hypoxia and a quenching effect of the molecule were evidenced. At the secretome level, the molecule downregulated IL-6,

Abbreviations: ECs, endothelial cells; G-CSF, granulocyte colony-stimulating factor; GSH, reduced glutathione; GSSG, oxidized glutathione; HIF-1α, hypoxia-inducible factor-1α; HSCs, hematopoietic stem cells; HUVEC, human umbilical endothelial cells; IL-6, interleukin 6; IL-8, interleukin 8; IP-10, interferon-γ induced protein 10; MCP-1, macrophage chemoattractant protein 1; MEA, S-acetyl-β-mercaptoethylamine; NAC, N-acetyl-cysteine; NAD, nicotinamide adenine dinucleotide; NADP, nicotinamide–adenine–dinucleotide phosphate; PDGF-BB, platelet-derived growth factor-BB; PRDX, peroxiredoxin; ROS, reactive oxygen species; TRX, thioredoxin; TRXR, thioredoxin reductase; VEGF, vascular endothelial growth factor.

MCP-1, and PDGF-bb. These results suggest that redox modulation by I-152 reduces oxidative stress and ROS level in hypoxic ECs and may be a strategy to fine-tune the environment of an *in vitro* BM niche able to support functional HSC maintenance.

KEYWORDS

antioxidant, endothelial cells, glutathione, hypoxia, I-152, redox, ROS, thioredoxin

1 | INTRODUCTION

Endothelial cells (ECs) are ubiquitously present across the vascular beds in the body. They represent the interface through which blood and neighboring tissue communicate via cytokine signaling, metabolites, and the exchange of gas and nutrients.[1] Their properties are tightly linked to their location due to physical and biochemical changes in the microenvironment.[2,3] In the arteries, blood flow guarantees proper oxygen (O_2) supply, whereas within the bone marrow (BM), in the proximity of sinusoids, low O_2 is physiologically needed for the maintenance of hematopoietic stem cell (HSCs) proliferation and differentiation. This low oxygen state (<5% O_2) with respect to 21% atmospheric O_2 is known as physiological hypoxia or physisoxia.[4] The BM is considered a tissue with a limited oxygen supply, and one of the hallmarks of the HSC niche is its low oxygen tension, hence the term "hypoxic niche." Direct *in vivo* measurements of local oxygen tension (pO_2) have determined the absolute pO_2 of the bone marrow as <32 mmHg.[5]

The BM comprises specialized regions with several cell types, such as the endosteal niche featuring cell members like osteoblast, adipocytes, and osteoprogenitor cells, and the vascular niche comprising immune cells, stromal cells, megakaryocytes, and ECs.[2] *In vivo*, there is fine-tuned balance between O_2 concentration and cellular cross-talk among the niche members, however, the same does not happen in the *in vitro* condition. *In vitro* hypoxic cultures with 1%–3% O_2 have been shown to promote HSC differentiation into multiple hematopoietic lineages, forgoing their stemness and self-renewability.[6,7] Low levels of reactive oxygen species (ROS) are linked to HSCs with high regenerative potential while increased ROS lead to their differentiation and exhaustion.[8,9] Previous studies using low O_2 with ECs highlighted how hypoxia (<5% O_2) decreased their viability, induced oxidative stress, and angiogenesis in a time- and O_2-dependent manner, through a strong increase in hypoxia-inducible factor α (HIF-1α).[10,11] Under normoxic conditions (>5% O_2) HIF1-α is negatively affected via continuous proteolytic degradation.[12,13]

However, in a hypoxic environment, HIF-1α regulates the transcription of hypoxia-responsive genes such as the vascular endothelial growth factor (VEGF), responsible for angiogenesis, and switches cells from oxidative to glycolytic metabolism to reduce ROS generation.[14,15] However, the concentration of ROS, such as superoxide and H_2O_2, is generally increased in ECs during hypoxia together with nitrogen species.[16,17] Attenuation of EC ROS levels and oxidative stress is desirable in the context of recreating an in vitro BM model aimed to maintain HSC proliferation capacity and stemness. This work investigated how redox modulation could influence the parameters involved in the *in vitro* response to hypoxia of ECs, which are one of the pivotal elements of the vascular BM niche. The response to low O_2 was explored using human umbilical endothelial cells (HUVEC) whose redox status was regulated by a molecule, named I-152, able to release NAC (N-acetyl-cysteine), a precursor of L-cysteine, and cysteamine (MEA).[18] Both NAC and MEA, administered singularly, were found to increase intracellular glutathione (GSH) levels[19,20]: NAC by providing a source of cysteine, whereas MEA breaking down cystine into cysteine and cysteine–cysteamine disulfide.[21,22] The tripeptide GSH (consisting of glutamate–glycine–cysteine) is considered a major reducing agent with a key role in protection against ROS damage and I-152 has been demonstrated to increase/restore GSH content more efficiently than NAC or MEA singularly or administered combined, both in vitro and in vivo.[23–25] Indeed previous studies demonstrated that the GSH-boosting effect of I-152 could be the result of a dual mechanism: by providing precursors for GSH synthesis (cysteine) and by inducing de novo GSH synthesis through the activation of the erythroid 2-related factor (Nrf-2) transcription factor.[24–26] GSH has a relevant role in the maintenance of cellular redox homeostasis being the ratio between its reduced state (defined so far as GSH) and oxidized form (GSSG) a key indicator of oxidative stress in combination with the redox couples $NAD^+/NADH$ and $NADP^+/NADPH$.[27,28] Similarly to the GSH system, other redox regulators are targets of the Nrf-2-antioxidant response element (ARE) signaling pathway, such as thioredoxin (TRX), thioredoxin-reductase (TRXR), and peroxiredoxins (PRDX).[29,30] PRDX proteins can reduce

peroxide and superoxide, providing a scavenging effect on ROS under oxidative stress.[31,32] Therefore, the activation/regulation of these systems is of increasing interest for tuning the hypoxia-induced redox responses thanks to the application of antioxidant molecules able to sustain redox homeostasis and providing desirable conditions *ex vivo* for engineering the BM niche, which so far has not been successful with respect to HSC proliferation and potency maintenance.

2 | EXPERIMENTAL PROCEDURES

2.1 | I-152 preparation

I-152 is a conjugate of NAC and *S*-acetyl-β-mercaptoethylamine (MEA) linked together by an amide bond and was synthesized as recently described.[33] In their work, Bartoccini and colleagues represented on Supporting Information p. S11 (compound 6) characterization data for I-152, including ^{1}H-NMR and ^{13}C-NMR.[33]

Contact for reagents and resource sharing: Francesca Bartoccini (francesca.bartoccini@uniurb.it).

2.2 | Cell culture

HUVEC were purchased from Lonza (Switzerland) and cultured in endothelial growth medium 2 (EGM-2™) supplemented with EGM-2 BulletKit™ (Lonza) to be used between passages 4–7. The experiment involved three groups: (1) normoxia (21% O_2), (2) hypoxia (3% O_2), and (3) hypoxia + I-152 treatment (3% O_2).

Untreated cells were set in the Hypoxia Chamber (StemCell Technologies) and flushed with 3% O_2, 92% N_2, and 5% CO_2 gas mixture for 15 min before being placed in a humidified incubator (37°C, 5% CO_2) for 1, 6, and 24 h. In the treated group, I-152 (0.03 mM) was added to the cell medium right before hypoxia. Sister culture, used as the control group, was left in the cell incubator at 21% O_2 for an equal time.

2.3 | Glutathione and thiol group detection

HUVEC (1×10^6 cells/flask) were lysed with 100 μL of lysis buffer (0.1% Triton X-100, 0.1 M Na_2HPO_4, 5 mM EDTA, pH 7.5) followed by 15 μL of 0.1 N HCl and 140 μL of precipitating solution [100 mL containing 1.67 g (w/v) of glacial metaphosphoric acid, 0.2 g (w/v) of disodium

EDTA and 30 g (w/v) of NaCl]. After centrifugation, pellets were resuspended in 100 μL 0.1 N NaOH, and proteins were quantified via Bradford assay (Bio-Rad). 25% (v/v) Na_2HPO_4 0.3 M and 10% (v/v) DTNB were added to the supernatants for thiol determination by HPLC through a BDS Hypersil™ C18 column (5 μm, 150 × 4.6 mm; Thermo Scientific). Separation and elution conditions were previously described elsewhere.[34,35] Following the detection at 330 nm, quantitative measurements were compared with known concentration standards and normalized to the protein content.

2.4 | Metabolomic study

HUVEC were seeded in technical duplicate at 5×10^6 cells per T75 flask for each condition: normoxia, hypoxia ± I-152. After 6 and 24 h, cells were washed with ice-cold PBS and subsequently harvested in cold 80/10/10 LC/MS grade methanol/acetonitrile/water (Carl Roth, Germany). Insoluble material was pelleted by centrifugation at 20,000 g for 20 min. In order to maintain redox-sensitive metabolites, buffers for extraction followed previously published protocols.[36]

The resulting supernatants were evaporated and pellets dissolved in 350 μL of 50/30/20 LC/MS-grade methanol/acetonitrile/water containing formic acid 0.1%. The supernatant was analyzed with ultra-high-pressure liquid chromatography Vanquish UHPLC system (Thermo Fisher Scientific) coupled to mass spectrometry (Exploris 240 Thermo Fisher Scientific). Briefly, compounds were separated by C18 Hypersyl GOLD column (150 × 2.1 mm × 1.9 μm, Thermo Fisher Scientific) using an aqueous phase (A) of water/0.1% formic acid and a mobile phase (B) acetonitrile/0.1% formic acid at 300 μL/min and 40°C. Compounds were also resolved by amide-HILIC Column (150 × 2.1 mm 2.6 μm) at 400 μL/min at 50°C, by using phase (A) of acetonitrile/water 95/5 containing 10 mM ammonium formiate/0.1% formic acid, and aqueous phase (B) 10 mM ammonium formiate/0.1% formic acid. Acquisitions were performed in positive and negative ion polarity modes. The Exploris 240 was set in MS1 range 80–900 m/z, 120,000 resolution at m/z 200, ACG target 10e6, and auto maximum injection time. For MS2, auto m/z range, stepped HCD normalized collision energy (20%, 50%, 80%, and 150%), 30,000 resolution at m/z 200, ACG target 2e5, and maximum injection time 70 ms. Calibration was performed prior to each analysis sequence, and moreover, the internal calibrant was employed in each run. The untargeted metabolomics was performed by using the deep scan AcquireX

software, with 5 ID runs, 5 quality control, and 3 replicates of each sample for statistical analysis. Raw data were processed by Compound Discoverer software Ver 3.3 (Thermo Fisher Scientific). Metabolite variations were set with a fold change of 1.5 and FDR < 0.05. Most significant metabolites were determined by the program and further analyzed manually.

2.5 | Real-time PCR

Total RNA (from 0.5×10^6 cells/flask) was extracted at 6 and 24 h with RNeasy Plus mini kit (Qiagen, Germany) after cell lysing with RLT buffer supplemented with 1% β-mercaptoethanol (Sigma, Germany). According to the manufacturer's instructions, the cDNA was synthesized using the Takara PrimeScript™ RT Mastermix (Takara, Japan) from 0.25 μg total RNA. The real-time PCR reactions were performed with ABI Prism 7500 Sequence Detection System (Applied Biosystems) in triplicate, using PowerUp® SYBR Green Mastermix (Applied Biosystems). The amplification conditions were 40 cycles at 95°C for 10 min, 95°C for 10s, and 60°C for 50s. Relative mRNA expression was determined with the $2^{-\Delta\Delta Ct}$ method using β-actin as a reference.

2.6 | Released cytokines determination

Cells supernatants of HUVEC were collected at 24 h, during the processing for the metabolic study (described in Section 2.4) and spun down at 10,000g for 10 min at 4°C to remove any cell debris and stored at −80°C until analyses. The human 27-plex kit was purchased from Bio-Rad and used according to the manufacturer's recommendations. The kit permitted the detection of the following cytokines: FGF basic, Eotaxin, G-CSF, GM-CSF, IFN-γ, IL-1β, IL-1ra, IL-2, IL-4, IL-5, IL-6, IL-7, IL-8, IL-9, IL-10, IL-12 (p70), IL-13, IL-15, IL-17A, IP-10, MCP-1, MIP-1α, MIP-1β, PDGF-BB, RANTES, TNF-α, and VEGF.

Plates were read using a BioPlex® 200 instrument (Bio-Rad), and interleukin concentrations (expressed as picograms per milliliter) were calculated by use of a standard curve and software provided by the manufacturer (Bio-Plex manager software, v.6.1) and normalized by protein content defined with Bradford assay.

2.7 | Proteomic investigation

Proteins from cells, prepared as previously described in Section 2.4, were processed by EasyPep MS Sample Kit (Thermo Scientific Pierce). Samples were dissolved in water 0.1% formic acid and 500 ng injected in an UltiMate 3000 RSLC nano system coupled to the Exploris 240 mass spectrometer. Briefly, peptides were desalted online by Acclaim PepMap C18 Reversed Phase HPLC Column (5 μm, 0.3 mm × 5 mm, Thermo Scientific), and then resolved by Easy-Spray Pepmap RSLC C18 (2 μm, 25 cm × 75 μm) at a flow rate of 300 nL/min with a gradient of phase B (80% acetonitrile/0.1% formic acid, solvent A was 0.1% formic acid in water) from 2% to 50% in 200 min. Then (B) was changed up 99% in 20 min, kept for 14 min, and then the column was re-equilibrated for 10 min. Data were acquired in a positive mode and data-dependent manner. For MS1 m/z range was set to 350–1500 at 120,000 resolution (at m/z 200), ACG target 3e6, and auto maximum injection time. MS2 was adopted when ions intensity was above 5e3, with m/z range in auto mode, normalized HCD energy 30%, ACG target 7.5e4, and maximum injection time 40 ms. The resolution was set to 15,000 at m/z 200 and the internal calibrant for employed in run start mode. Samples were analyzed in quintuplicated and raw data employed in Proteome Discoverer software v2.5 adopting the label-free signal quantification strategy. Master proteins were considered differentially expressed with a fold change 2 and FDR < 0.05.

2.8 | Western blot

Cells were lysed in Sodium Dodecyl Sulfate (SDS) buffer [50 mM Tris–HCl, pH 7.8, 0.25 M sucrose, 2% (w/v) SDS, 10 mM N-ethylmaleimide-NEM] supplemented with a cocktail of protease (Complete, Roche) and phosphatase inhibitors (1 mM Na_3VO_4, 1 mM NaF). Lysates were boiled for 5 min, sonicated at 100 Watts for 40 s, and cleared by centrifugation at 12,000g. Protein content was determined by the Lowry Assay using bovine serum albumin (BSA) as a standard, resolved by SDS polyacrylamide gel electrophoresis (SDS-PAGE). and electroblotted onto polyvinylidene difluoride (PVDF) membranes (0.2 μm pore size). Before blocking in 5% (w/v) nonfat dry milk (Cell Signaling Technologies), membranes were labeled with No-Stain™ protein labeling reagent (Invitrogen) for total protein detection and visualization via a ChemiDoc MP Imaging System (Bio-Rad). Afterward, membranes were incubated with the following primary antibodies: anti-Thioredoxin 1 (C63C6, #2429), and anti-thioredoxin reductase (TRXR1, #6925) from Cell Signaling Technologies. After overnight incubation at +4°C, a horseradish peroxidase (HRP)-conjugated secondary antibody (Bio-Rad) was used and bands were visualized with the enhanced chemiluminescence detection kit WesternBright

ECL (Advansta) in ChemiDoc MP and quantified by using the Image Lab software (Bio-Rad).

2.9 | ROS evaluation

The ROS-ID® Hypoxia/Oxidative stress detection kit (Enzo Life Sciences) was used according to the manufacturer's protocols to evaluate the total ROS production induced in hypoxic cells with decreasing concentrations of I-152 (0.125, 0.06, and 0.03 mM). HUVEC were seeded with a density of 0.01×10^6 cells/well in a 96-well plate. Cells were incubated with or without the compound at 3% O_2 for 1, 6, and 24 h in Clariostar plus microplate reader (BMG Labtech, Germany).

The level of ROS, namely hydrogen peroxide (H_2O_2), peroxynitrite ($ONOO^-$), and hydroxy radical ($^•OH$), was determined at the microscope Evos M5000 (Thermo Fisher Scientific) via GFP filter (Ex./Em. 470/525) whereas hypoxic cells were acquired via Texas red filter (Ex./Em. 585/628).

2.10 | Statistics

Statistics and graphical representations were performed using GraphPad Prism™ 9. Data are expressed as the means $\pm$ SD of three experimental groups. Differences between the experimental groups were analyzed using an unpaired two-tailed Student's t-test and Welch's t-test. Results were considered statistically significant for $p < 0.05$. Quantitative analyses of the images were accomplished with ImageJ.

3 | RESULTS

In this work, we described an EC culture model in hypoxic conditions *in vitro* and how redox modulation, via I-152, a drug-releasing NAC and MEA, affects the cellular metabolic/proteomic profile and oxidative responses. Previous studies have established glutathione levels and anaerobic metabolism in hypoxic models[37,38]; however, we implemented a redox regulator (I-152) in order to unravel the impact of redox influence in ECs facing the hypoxic system (3% O_2).

3.1 | Glutathione detection

To define the ideal concentration of I-152, a dose–response curve was performed within the previously established nontoxic range (0.25, 0.125, 0.06, and 0.03 mM).[39] Based on the sustained GSH production, 0.03 mM was determined to be the best concentration providing a statistical increase after 6 and 24 h (Figure 1A).

Further analysis of the free thiol pools by HPLC showed that I-152 increased intracellular levels of other forms of thiols (Figure 1B). Particularly NAC and MEA were detected in all the treated groups in a dose-dependent manner until reaching the instrument detection limit at the concentration of 0.06 mM. Although I-152 is expected to liberate equimolar concentrations of NAC and MEA, intracellular MEA levels were lower than those of NAC, suggesting that MEA could be partially converted into cystamine upon oxidation of its sulfhydryl group and/or form mixed disulfides.[21] Such disulfides could not be revealed by the chromatographic analysis used here since it was specific for the identification of –SH-carrying molecules. I-152 was not measured by this analytic system probably due to the instrument detection limit, although it was quantified by mass spectrometry analysis as reported subsequently.

To assess the redox perturbation induced by hypoxia and the modulatory effect of the pro-drug I-152, GSH content was determined in HUVEC maintained in hypoxic conditions treated or not with the molecule (Figure 1C). Considering that *in vivo* the BM niche is a hypoxic environment with oxygen varying from 5% to 1% towards the sinusoids, cells were inserted in a hypoxic chamber containing 3% O_2 and 5% CO_2 (with a presumptive calculated pressure of ~22 mmHg) and kept in the incubator at 37°C for 1, 6, and 24 h. The following groups were tested in these settings: normoxia, hypoxia, and hypoxia +0.03 mM I-152. Figure 1C highlights how hypoxia reduced intracellular GSH at 1, 6, and 24 h, whereas the application of I-152 replenished GSH content towards the normoxic level (Control) at 6 and 24 h. In order to assess whether I-152 had an effect on GSH by providing cysteines in a similar manner as NAC, cells were treated with 0.03 mM of NAC and kept in hypoxia for 6 h. Results (Figure S1) highlighted how GSH and cysteine content with both I-152 and NAC was superior to that of hypoxic cells. However, GSH in I-152-treated cells was increased compared to those having received NAC, suggesting that I-152 may augment GSH content through different mechanisms, as previously reported.[25]

3.2 | Metabolomic study

An untargeted metabolomic study via mass spectrometry was applied to investigate the complete hypoxia-dependent profile and the possible modifications due to the I-152 treatment. To examine the metabolic profile of
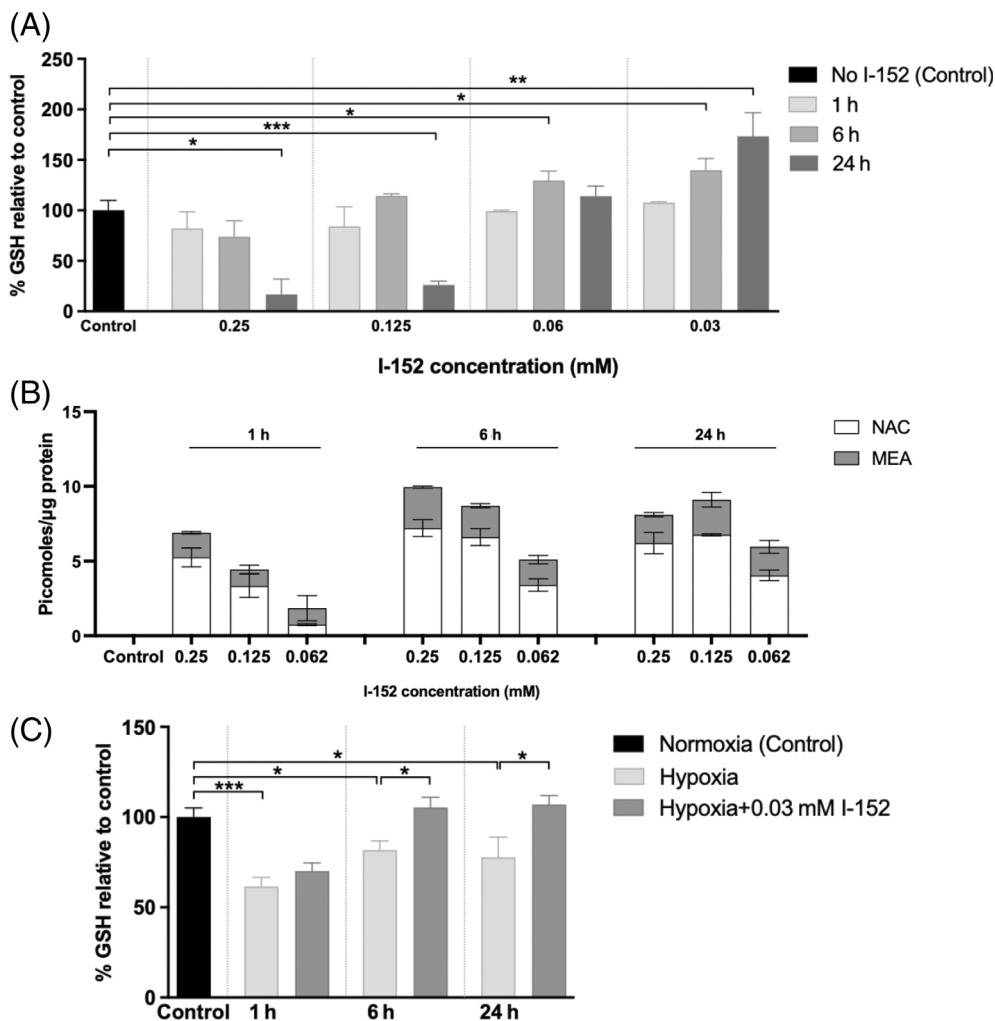
FIGURE 1 (A) GSH content in HUVEC at 21% O_2 treated with decreasing concentrations of I-152 for 1, 6, and 24 h. GSH is expressed as a percentage with respect to untreated cells (Control). An I-152 concentration of 0.03 mM was chosen for further experiments. (B) Metabolites of I-152: N-acetyl-cysteine (NAC) and cysteamine (MEA) were found within HUVEC cells after 1, 6, and 24 h of treatment at 21% O_2. None of those compounds were found in the untreated group (Control). Metabolites are expressed as picomoles/μg of protein and plotted values are the mean $\pm$ SD of two separate experiments. (C) GSH content in HUVEC set in hypoxia (3% O_2) and treated with 0.03 mM of I-152 for 1, 6, and 24 h. GSH is expressed as a percentage with respect to untreated cells in normoxia (21% O_2; Control). Plotted values are the mean $\pm$ SD of two separate experiments. *p-value <0.05, **<0.005, ***<0.001. GSH and thiol levels were determined via HPLC and normalized on protein content.

the ECs exposed to hypoxia for 6 and 24 h, we used HILIC and C18 columns (both positive and negative for polar and apolar compounds, respectively).

The extraction buffer allowed the maintenance of redox-sensitive compounds[36] and the workflow, that was followed, enabled the detection of ~20,000 metabolites, among those, 1501 were identified.

The metabolic profile under hypoxia was compared firstly with the normoxic control and secondly with I-152-treated hypoxic cells. The complete listing of hypoxia-dysregulated metabolites has been included in Supporting Information S2 and a graph illustrating the polarity of the analyzed metabolites has been incorporated in Figure S3A.

The PCA representation, in Figure 2, shows how the treatment group presents some intermediate values between the normoxic control profile and the hypoxic one, partially restoring or maintaining certain polar and apolar metabolites at both 6 h (Figure 2A) and 24 h (Figure 2B) suggesting a slower progression of the cells toward the hypoxic profile. The specific I-152 mass spectrum was also detected and implemented in Figure S3B.

Besides PCA representations, heatmaps of the changes in metabolites related to hypoxia and the profile of I-152-treated cells were portrayed in Figure S4. Further analysis of single redox-related metabolites was performed and illustrated in Figure 3. It is possible to observe that, the majority of these metabolites, such as
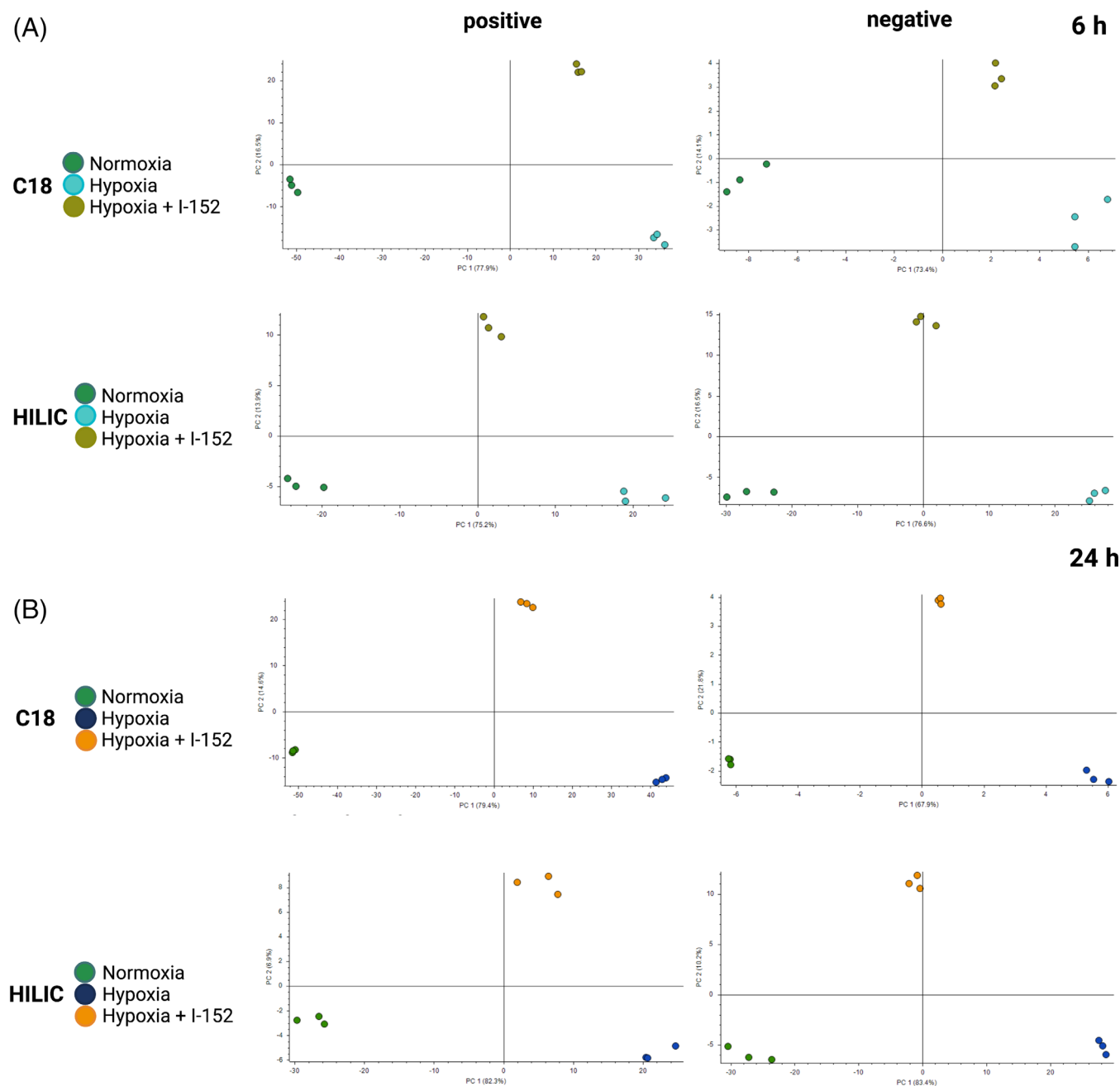
FIGURE 2 PCA graphics representing HUVECs in normoxia or in hypoxia after 6 h (A) and 24 h (B). The cells, kept in hypoxic conditions, were treated or not with I-152 at the concentration of 0.03 mM. Metabolites were detected using HILIC and C18 columns in positive and negative for polar and apolar metabolites and measured by LC–MS/MS. Plots are the results of three biological replicates.

GSH, GSSG, creatine, creatinine, s-adenosylmethionine, cystathionine, and glutamate, was downregulated in hypoxia at both time points (depicted in green), while only a few (ornithine and ADP) were upregulated (depicted in red). Most of these effects were counterbalanced by the I-152 treatment as shown in C and D where the same color pattern (green and red) is maintained.

The hypoxic profile matched those of previous metabolomic studies described by other groups with respect to redox metabolites.[38,40] Therefore, narrowing down to the

main redox couples, that is, GSH, GSSG, $NAD(P)^+$ $NAD(P)H$, the results of the untargeted analysis were reported as fold changes in Figure 4. With respect to glutathione levels, I-152 raised GSH after 6 and 24 h, mirrored by a related increase in GSSG at both time points with respect to hypoxia.

Besides GSH and GSSG, the redox couples $NAD(P)^+/$ $NAD(P)H$ were also evaluated as essential for redox homeostasis and cell metabolism.[41] These data portrayed a shift to the oxidative state, in particular with regard to
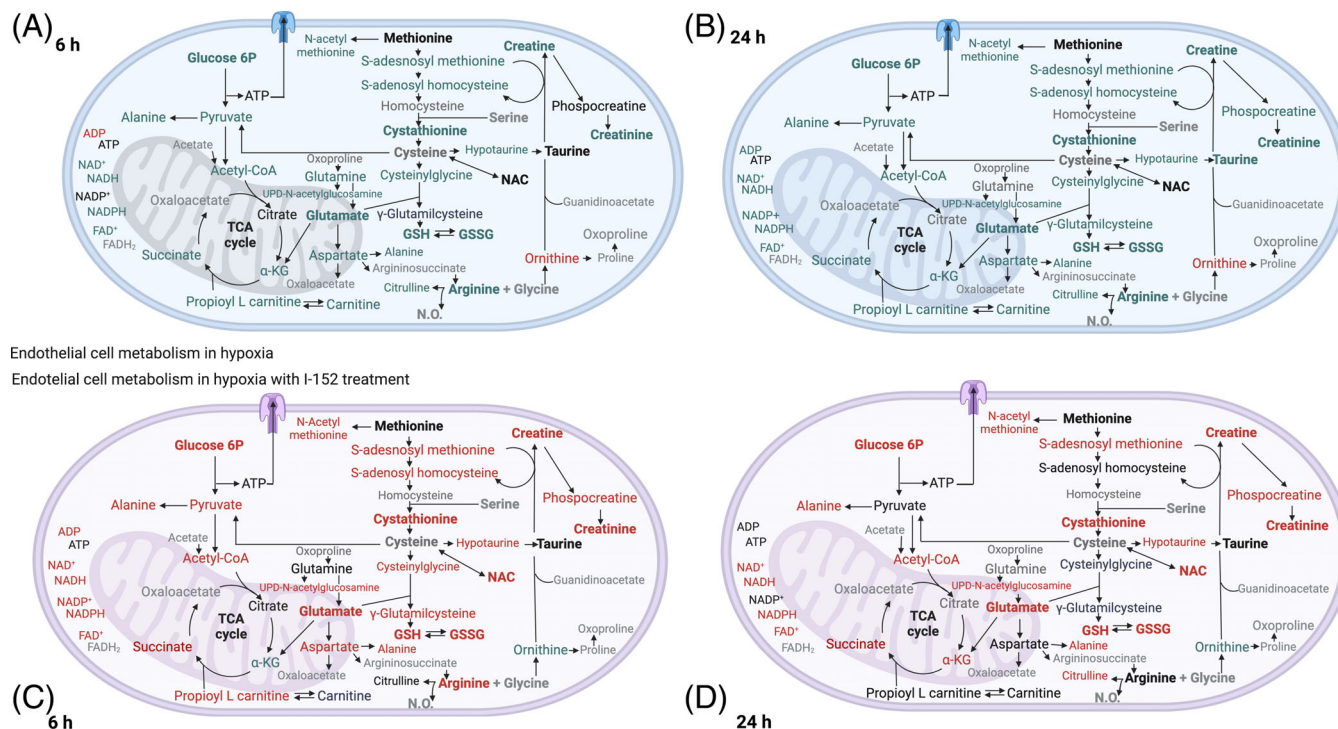
FIGURE 3 Metabolic pathway network map of HUVEC maintained in hypoxia for 6 (A) and 24 h (B) and hypoxia plus I-152 (C, D). The downregulated metabolites are shown in green, the upregulated ones in red, the not detectable ones in gray, and those that do not statistically change (considering normoxia vs. hypoxia and treated group vs. hypoxia) in black.

the couple $NAD(P)^+/NAD(P)H$ due to hypoxia, and a reductive shift in the treated group. However, only a targeted analysis with the use of internal standards would allow quantification and direct redox-couples ratio calculation.

De novo NAD^+ synthesis from tryptophan can be achieved via the kynurenine pathway where the amino acid is converted to N-formyl kynurenine and kynurenine in the first steps.[42] Hypoxia depicted a reduction in tryptophan in favor of kynurenine at 6 and 24 h. However, in the treated group, tryptophan consumption was more moderate and kynurenine quantity was low at both time points suggesting that tryptophan usage for this route was unlikely (Figure 4A). A subsequent proteomic study revealed that only the cytosolic isocitrate dehydrogenase that converts NAD^+ into NADH was upregulated versus hypoxia, whereas malate dehydrogenase was not altered in comparison with the hypoxic group in cytosol suggesting that I-152 partially influenced the formation of NAD(P)H through the synthesis of that dehydrogenase (Figure S7).

Hypoxic exposure induced a metabolic shift with a reduction of creatine and creatinine levels[43]; however, treatment with I-152 improved their content likely due to S-adenosylmethionine availability (Figures 3 and 4A). The creatine mechanism of action as an antioxidant is not known yet. However, it has been shown to be involved in vascular health by reducing ROS and free radicals, inflammation, and circulating homocysteine, parameters closely linked to vascular disease.[44–46]

I-152 itself and one of its metabolites (NAC) were found within the cells only in the treated groups supporting previous findings[25] and those reported in the present manuscript: aforesaid compound's ability to cross the membrane and release the parent compounds (Figure 4B). The increased presence of N-acetyl groups was also mirrored by increased N-acetyl-methionine, N-acetyl-glutamate, and UDP-N-acetyl-glucosamine (UDP-GlcNAC), which is required for protein N- and O-linked glycosylation and crucial for protein function (Figure S2).

3.3 | Gene expression

In previous studies conducted by our group with HUVEC maintained in anoxia (<1% O₂), transcriptomic analysis revealed that among the dysregulated genes during the O₂ deprivation, particularly Hypoxia-inducible factor 1α (*HIF-1α*) and HIF-1α-dependent angiogenic factors like the vascular endothelial growth factor (VEGF) emerged.[47] Therefore, RT-PCR was used to determine the gene expression of *HIF-1α*, *VEGF*, and the Thioredoxins (*TRX-1 and 2*), in hypoxic vs normoxic cells (Figure 5).
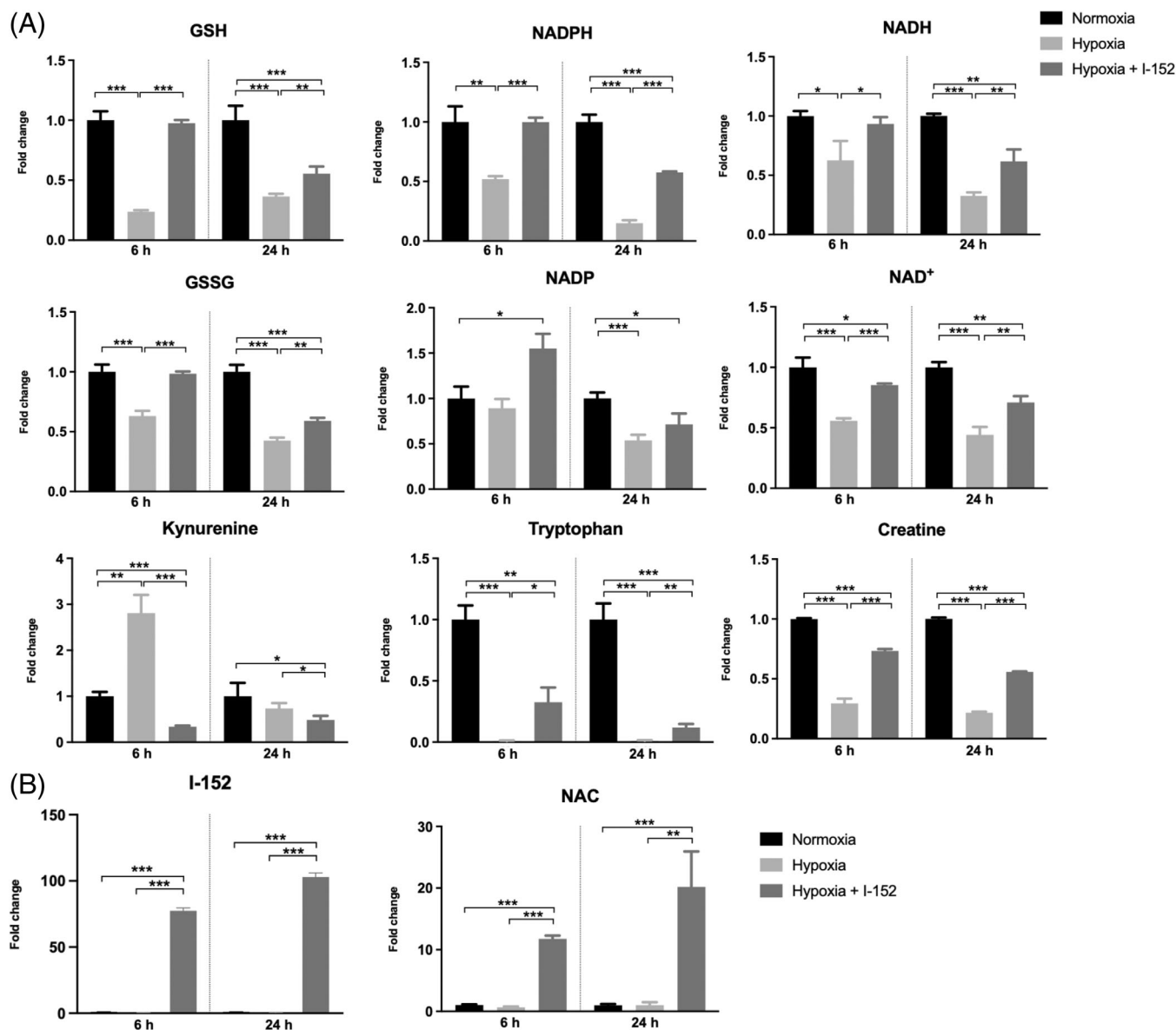
FIGURE 4 (A) Highlights of a few significantly altered metabolites belonging to the redox system in HUVEC in hypoxia $\pm$ I-152 vs the normoxic control. (B) I-152 and N-acetyl-cysteine (NAC), which is a by-product generated from the compound metabolism within the cell, are highly present in the treated group. Plotted values are the mean $\pm$ SD of three experiments and *p-value < 0.05, **<0.005, ***<0.001.

HIF-1α is the inducible subunit of the HIF-1 transcription factor, that regulates those genes involved in the response to hypoxia.[48] VEGF is one of the genes upregulated by HIF-1 and is the primary cytokine related to angiogenesis.[49] TRXs are a family of redox-active proteins involved in the antioxidant defense response complementing the GSH system in protection against oxidative stress.[50] The upregulation of *HIF-1α* at 6 h was mirrored by increased *VEGF* at 24 h, and in parallel, the downregulation with I-152 at 6 h was followed by a lower *VEGF* expression at 24 h. While TRX 1 is located in the cytosol and TRX 2 in the mitochondria, they both share a role in regulating redox and NAD(P)H systems.[51] Results

showed that hypoxia did not affect *TRX 1* and *2* at the mRNA level at 6 h but only at 24 h a statistical reduction was observed, in particular in *TRX2* mRNA quantity. *TRX 1* and *2* mRNAs were significantly induced by the treatment at 6 h, then they decreased at 24 h and no statistical differences emerged in comparison with the hypoxic group.

3.4 | Secreted cytokines

The secretome profile of hypoxic cells $\pm$ I-152 after 24 h was compared with that of those kept in normoxic
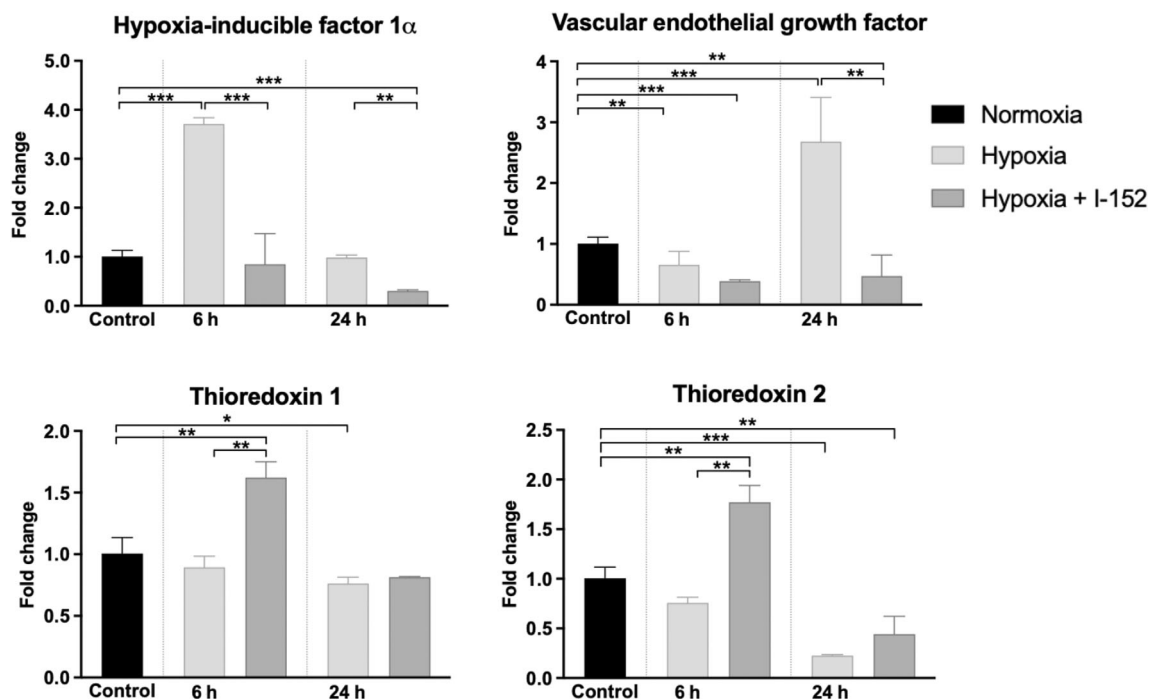
FIGURE 5 Gene expression profile of HUVEC in hypoxia treated or not with I-152 versus the normoxic control (Control) at 6 and 24 h. After total RNA extraction and cDNA synthesis, relative mRNA expression was determined by real-time PCR with the ΔΔ-Ct method using β-actin as a reference gene. Plotted values are the mean ± SD of three separate experiments. *p-value < 0.05, **<0.005, ***<0.001.
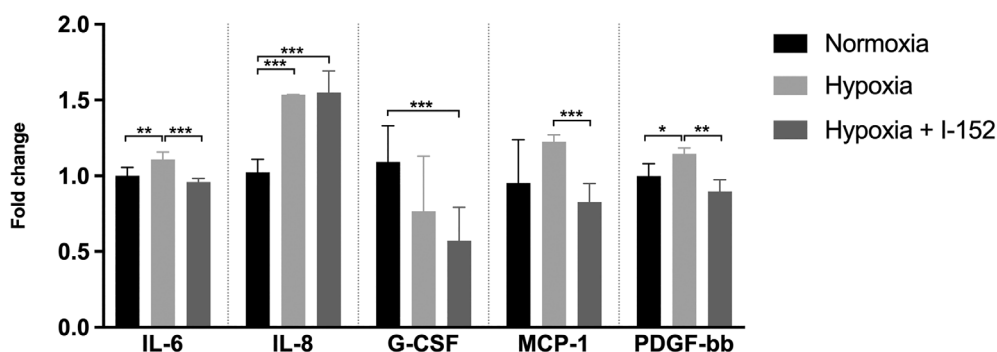

FIGURE 6 Cytokines secreted by HUVEC after 24 h in hypoxia ± I-152 treatment vs the control (Normoxia). Cytokines, detected via Bioplex array, were evaluated as pg/ml and normalized on the protein content. The graph expresses the fold change with respect to the normoxic control. Plotted values are the mean ± SD of three experiments and p-value *<0.05, **<0.005, ***<0.001.

condition (Figure 6) via a 27-plex detection kit. The analysis revealed that only a few cytokines analyzed were secreted by the cells and VEGF had to be excluded for being part of the EGM-2 medium. We could observe that the increased secretion induced by hypoxia of interleukin-6 (IL-6), macrophage chemoattractant protein-1 (MCP-1), and the platelet-derived growth factor (PDGF-bb) was hindered by the treatment, whereas interleukin-8 (IL-8) and granulocyte-colony stimulating factor (G-CSF) secretion was unaffected by the redox alteration. G-CSF and MCP-1 are responsible for the chemotaxis of myeloid and lymphoid together with mobilization and myeloid

differentiation of HSCs.[52,53] Similarly, PDGF-bb is also known to be involved in HSC activation and chemotaxis.[54]

3.5 | Proteome study

Besides the hypoxia-altered secreted cytokines, a proteomics study was performed to evaluate possible intracellular changes in protein levels.

Proteomics analysis identified a total of 10,128 proteins (including isoforms) and 1292 master proteins (excluding isoforms). Among these, 262 were affected by
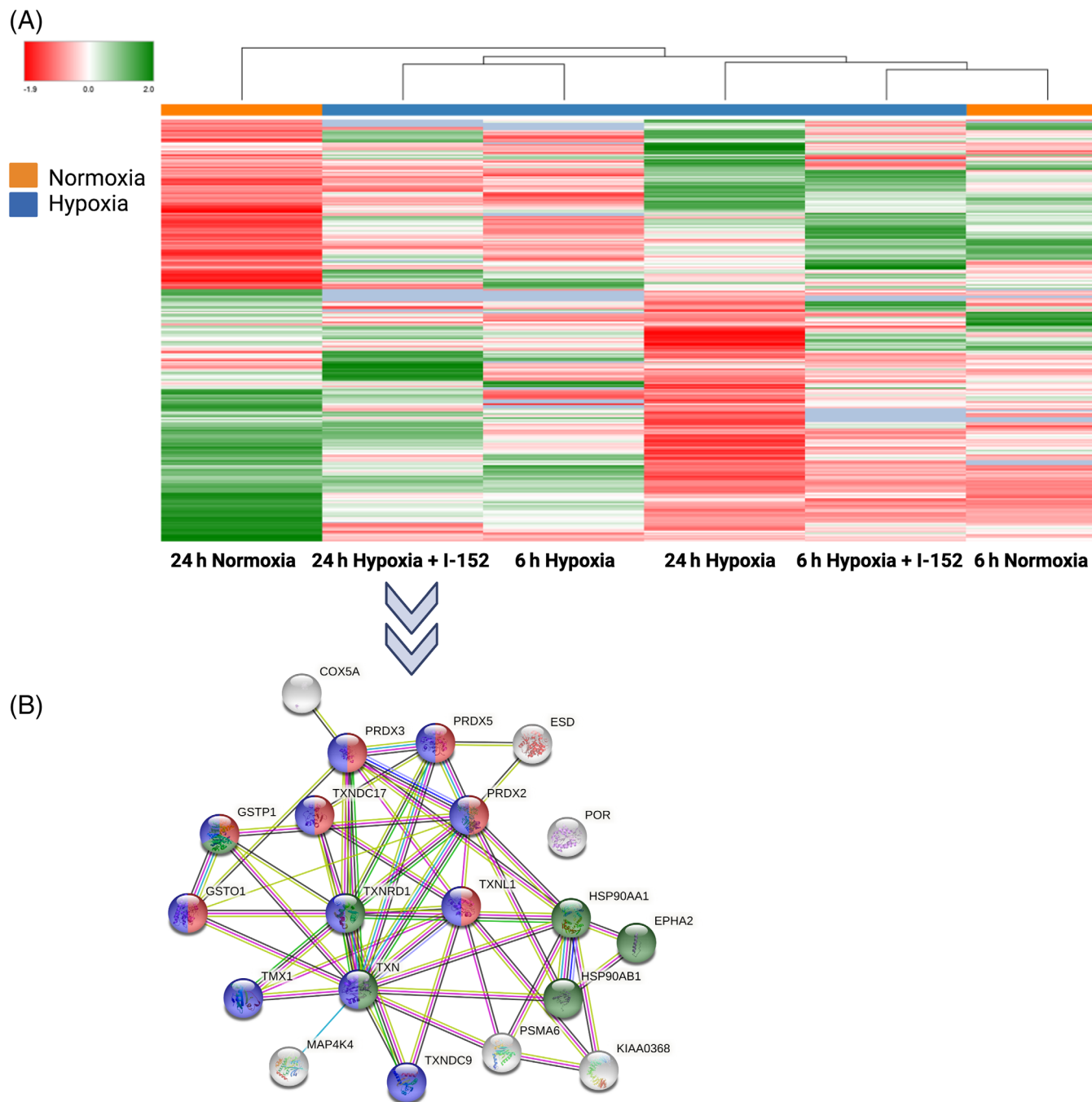
FIGURE 7 (A) The heatmap represents the proteins from HUVEC statistically dysregulated by hypoxia (3% of O_2), quantified via a proteomic assay with a fold change over the control by >2 and <0.5 and normalized to cell number. The green shaded region indicates upregulated proteins whereas red depicts the downregulated ones. "T" marks the treatment groups. The evaluation was performed with Proteome Discoverer™. (B) Schematic protein–protein interaction networks of hypoxia-downregulated redox-related proteins that are statistically upregulated by I-152 in hypoxia after 24 h. HUVEC cells were kept in hypoxia for 24 h before the analyses. Data were visualized in STRING (v.11.5), where nodes (circles) represent the protein with the connections between them. Each node color represents a different pathway class that belongs to the Thioredoxin superfamily (blue); Glutathione metabolism (red) and Nrf-2 pathway (green).

hypoxia at 6 h and 240 at 24 h. The 2-fold change was used to define proteins that were significantly upregulated or downregulated, respectively versus the normoxic control. In Supporting Information S5, a list of the modulated proteins has been provided.[55]

After proteome profiling using Proteome Discoverer©, the differentially expressed proteins were visualized in a heatmap (Figure 7A). The protein profiles were clustered using hierarchical clustering, which showed that at both 6 and 24 h, the I-I52 treated group has a closer proteomic
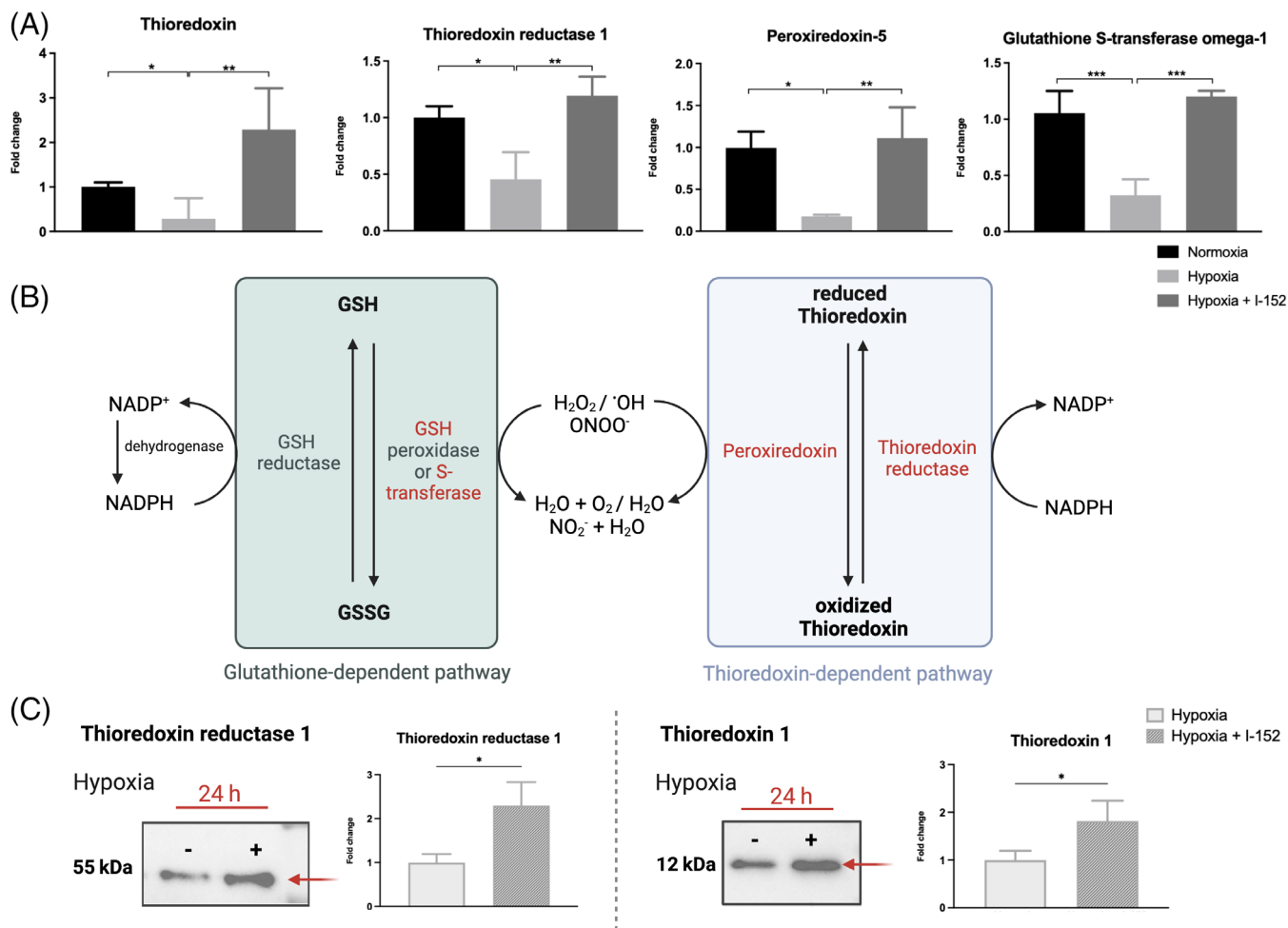
FIGURE 8 (A) Highlights of a few proteins in HUVEC modulated by hypoxia and I-152 after 24 h: thioredoxin, thioredoxin reductase-1, peroxiredoxin-5, GSH S-transferase Omega-1. Protein levels were evaluated via mass spectrometry-based proteomics and normalized over the total protein content. The value represents the mean value of the triplicate and is expressed as a fold change vs the control (normoxia). *p-value <0.05, **<0.005, ***<0.001. (B) Schematic view of the interconnection between glutathione and thioredoxin pathways and their common action on ROS. Glutathione (GSH) is an antioxidant that degrades hydrogen peroxide (H_2O_2) and hydroxyl radical ($\cdot$OH) via GSH peroxidase to water and peroxynitrite ($ONOO^-$) to nitrogen dioxide with GSH S-transferase.[59,60] Oxidized GSH (GSSG), is reduced back by GSH reductase in combination with NADPH. Similarly, peroxiredoxins oxidized thioredoxin while specific reductase returns the protein to its reduced form with NADPH.[61] The upregulated enzymes are highlighted in red. (C) Wester blots of Thioredoxin reductase 1 (left) and Thioredoxin 1 (right) from cells kept in hypoxia for 24 h treated (indicated with $+$) or not ($-$) with I-152, alongside their respective quantification plots confirming the proteomic results. Uncropped images and total protein labeling for normalization are illustrated in Supporting Information S8.

profile to that of the normoxic control. A PCA graph has been included in Figure S6.

Among all the proteins, the ones modulated by I-152 and belonging to the TRX family (e.g., TRX reductase), GSH metabolism (e.g., GSH-transferase), and the Nrf-2pathway (e.g., Heat-shock protein 90) were highlighted and represented by a specific color code via the STRING database (Search Tool for the Retrieval of Interacting Genes/Proteins)[56,57] (Figure 7B).

Both glutathione-dependent and thioredoxin-dependent pathways convert ROS to non-reactive species. The first one relays on GSH peroxidase and additionally

on GSH transferase to catalyze the reduction of peroxide-containing compounds (H_2O_2 and ROOH) but also superoxide ($O_2^{\cdot-}$), nitric oxide (NO), hydroxyl radical ($\cdot$OH), and peroxynitrite ($ONOO^-$).[58] Correspondingly, PRDX utilize thioredoxin (TRX) as a substrate to degrade peroxides and both GSH and TRX can be restored to their reduced form with the help of NAD(P)H. In order to further narrow down proteins that may have a pivotal role in this redox system, TRX, TRXR, PRDX-5, and GSH S-transferase have been represented in Figure 8A, which clearly shows that the hypoxic down-modulation was counteracted by the treatment with I-152. Their role in
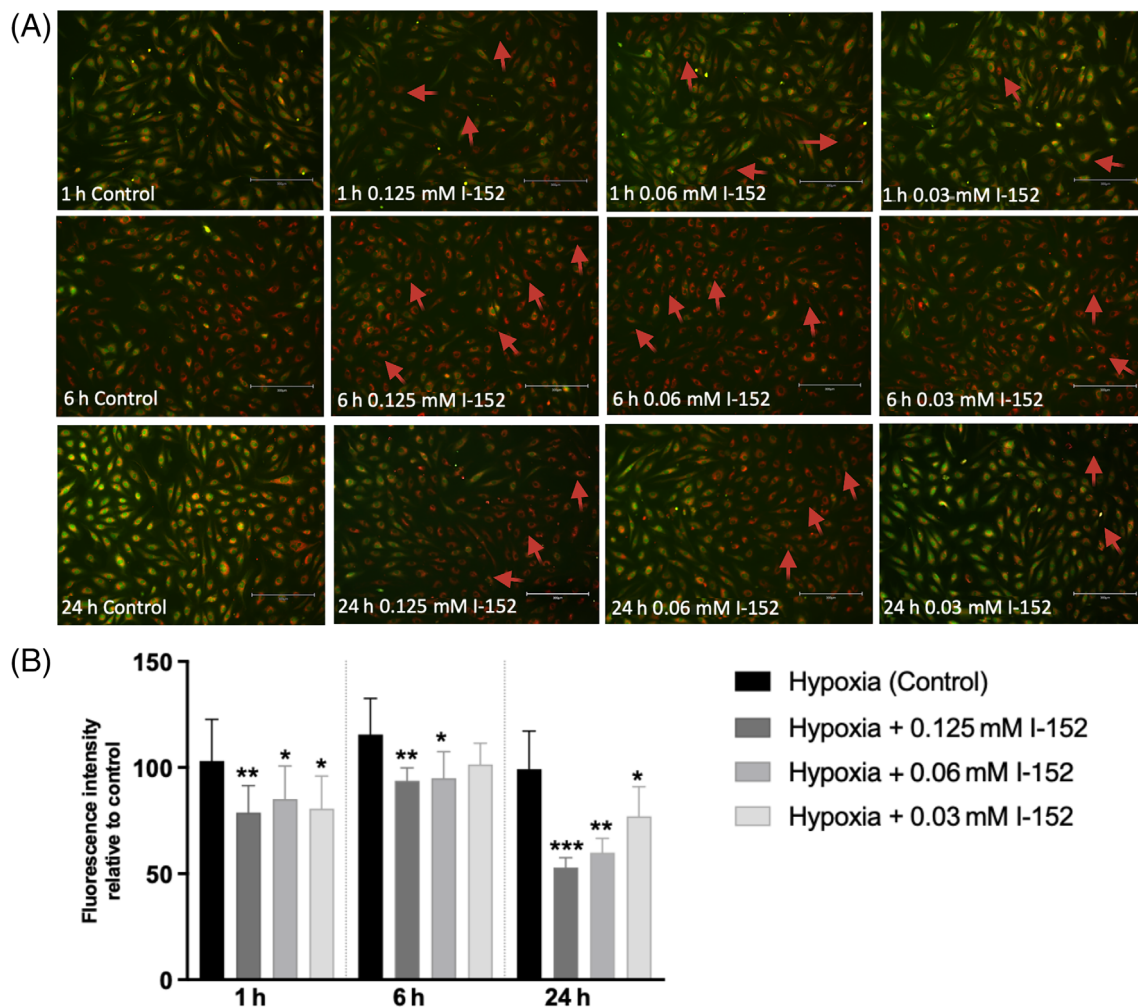
FIGURE 9 Reactive oxygen species (ROS) detection at 3% O_2 via fluorescence microscopy. (A) HUVEC were cultivated for 1, 6, and 24 h in hypoxia, and ROS were visualized using a ROS-ID® Hypoxia/Oxidative stress detection kit. The cells in hypoxia were compared with those treated with different concentrations of I-152 (0.125, 0.06, and 0.03 mM) in the same hypoxic condition. The kit can label simultaneously hypoxic cells (under 5% O_2) in red (pointed out by the red arrows) and ROS (specifically H_2O_2, ONOO– and •OH) with a green fluorophore. Magnification 10× (scale bar 300 μm) (B). Results of the semi-quantitative analyses were obtained using ImageJ. The graph represents the mean fluorescent intensity (green) relative to the hypoxic control and normalized to their internal control (red fluorescence). The value represents the mean value of six experiments ±SD and is expressed as a fold change vs the control (normoxia). *p-value <0.05, **<0.005, ***<0.001.

redox homeostasis in the presence of ROS is portrayed in Figure 8B. Western blots of TRX and TRXR confirmed the proteomic findings (Figure 8C).

3.6 | ROS evaluation

The generation of ROS under hypoxia is likely to alter intracellular redox status: specifically, ROS production affects the level or function of molecules that maintain the reducing environment of the cytosol,[28] as we could evaluate as well from the metabolic and proteomic studies.

Semi-quantitative fluorescence intensity analyses using ImageJ revealed ROS augmentation immediately after 1 h

of hypoxia and their quenching at 6 h, likely due to the cell antioxidant-triggered response. However, this condition was followed by a subsequent rise in ROS after 24 h of hypoxia. The treatment with I-152 dampened the hypoxia-induced ROS, particularly evident at 24 h (Figure 9B). Other quantification methods were not implemented in order to avoid cell re-oxygenation during processing.

4 | DISCUSSION

BM is composed of several cell lineages, including macrophages, mesenchymal stromal cells, ECs, HSCs, osteoblasts, monocytes, T-cells, and so forth, and is a tissue

essential for blood cell formation (hematopoiesis). In the BM cavity, it is possible to define distinctive niches permeated by decreasing concentrations of oxygen, from endosteal areas, closer to the bone, and arteriole-rich zones to the deep hypoxic sinusoids.[62] In the latter low oxygen levels are relevant for controlling the metabolism and cell fate of HSCs.[63,64] Characterization and collection of HSCs *in vivo* from the BM niche is still a challenge; therefore, there is a need to find *in vitro* culture conditions that support functional HSC growth.[65] When these cells are exposed to atmospheric levels of oxygen (∼21% O_2), HSCs rapidly begin the process of differentiation.[66] Likewise, in hypoxic conditions, the direct application of recombinant cytokines cocktails trying to mimic the BM micro-environment has limited success in HSC expansion.[67] Recent efforts have therefore focused on the use of cells, in co-culture with HSCs, able to sustain their maintenance *in vitro*.[68]

This study is focused on a pivotal component of the vascular system, the ECs, to investigate cellular behavior and the influence of redox modulation on cell metabolic activity/function.

ECs were set in hypoxia for different time points and combined with a redox modulator, I-152, a co-drug of NAC and MEA. The effects of hypoxic conditions on HUVEC have been already investigated and described in the literature,[69] and likewise the application of NAC and MEA separately in hypoxic studies *in vitro* and *in vivo*.[70–73] However, taking advantage of the ability of our molecule to release both compounds, overcoming their limitations, such as poor cellular uptake of NAC and MEA fast oxidation,[74,75] we wondered how I-152 could restore hypoxia-altered redox homeostasis in ECs.

In previous works, I-152 boosted intracellular GSH with higher efficiency compared to individually given NAC or MEA, by providing cysteine and conceivably by inducing Nrf-2 nuclear translocation,[25] although other molecular mechanisms behind the antioxidant effects of I-152 have not been excluded.[76] Indeed, such mechanisms may vary on the redox state of the cells (e.g., GSH-depleted ones or not) and the concentrations of the applied molecules (e.g., NAC concentration is usually administered above 1 mM). In this study, I-152 increased the tripeptide content at all the time points (1, 6, and 24 h) both in normoxic and hypoxic conditions. Thiol analyses in HPLC detected the presence of NAC and MEA within the cells, whereas mass spectrometry revealed also I-152 itself indicating the presence of the compound and its metabolic derivatives within the cells. Indeed, the addition of acetyl groups in I-152, enabled cell membrane permeation, even though a possible transporter-mediated uptake could not be excluded.

Besides GSH, the depletion of NADH and NADPH in hypoxia suggests a shift toward an oxidizing environment and I-152 appears to dampen this effect, partially thanks to increased Nrf-2-dependent isocitrate dehydrogenase.[77,78]

In parallel, *TRX-1* and *TRX-2* mRNA was overexpressed in the treatment group after 6 h. At the protein level, I-152 treatment resulted in increased expression of TRX-1, TRXR, and PRDX-5 at 24 h. These results could be correlated with the capacity of I-152 to activate Nrf-2 and its target genes *TRX-1* and *TRXR*,[25,30] suggesting that the molecule could tune not only the glutathione-dependent system but also other central antioxidant systems deputed to maintain redox homeostasis in mammalian cells. Redox regulation is essential for protection against oxidative damage, metabolism maintenance, and redox signaling,[79] therefore, functional glutathione and thioredoxin systems are crucial points during oxidative stress.

Such redox machinery facilitates the reduction of ROS by cysteine thiol-disulfide exchange[80] and, in our study, improvements of such systems via I-152 probably generated a more reduced environment within the cell, as reflected by the lower level of cellular ROS.

Moreover, in ECs, HIF-1α is the major mediator of the transient O_2-sensitive transcriptional response and of the downstream stress response signaling pathways.[81] Former studies described how NAC attenuated HIF-1α activation,[82] and we could hypothesize a similar effect in our settings.

A member of the HIF-dependent cascade, *VEGF*, which is involved in both angiogenesis and hematopoiesis,[83] was downregulated as well by the compound. Additionally, *VEGF* expression seems to be promoted in a paracrine manner by the hypoxia-upregulated IL-6.[84,85]

Observing then the secreted cytokines in our model, I-152 negatively influenced the production of IL-6, G-CSF, MCP-1, and PDGF-bb, which are all pro-inflammatory molecules. It was previously demonstrated that EC treatment with NAC inhibited the secretion of IL-6 in response to hypoxia, however, at the higher concentration of 1 mM.[86,87] Secreted G-CSF, MCP-1, and PDGF-bb are all differentiating agents of HSCs and while G-CSF regulates myelopoiesis at the expense of lymphopoiesis, PDGF-bb differentiates those cells triggering thrombopoiesis. Although the hypoxia-driven changes in cytokine production were minimal, the treatment restored the levels observed in normoxic controls. Keeping in mind the role of these cytokines in HSC differentiation, it could be of interest to examine further the biological significance.

So far, the proposed study investigated redox modulation of a single-cell type model in hypoxia. However, as mentioned previously, the BM niche is a complex system; therefore, co-culture studies with HSCs are highly desirable to portray the cross-talk among niche components and their effect on self-renewal/differentiation. Promising results obtained with I-152 treatment concerning GSH levels, ROS reduction, and secreted cytokines could help ECs to deal with hypoxia *in vitro* favoring a promising environment for HSC maintenance.

Hence, targeting the redox biology of ECs could be applied in future studies for HSC modulation with the final aim of recreating a full *in vitro* BM niche supporting HSC proliferation and stemness.

This work represents a comprehensive study of redox metabolic and proteomic changes making a step forward in the mechanistic aspects of hypoxic response in ECs. It is important to point out that O_2 deprivation, besides being a constituent of the BM niche, is also featured in several vascular diseases,[88] therefore, balancing the redox system in disease models associated with hypoxia-dependent altered redox mechanisms could represent another possible application to be considered.

5 | CONCLUSIONS

This work provides an overview of the redox alterations occurring in ECs in response to hypoxia and treatment with the pro-glutathione molecule I-152. Several metabolites and proteins involved in the glutathione–thioredoxin systems are found to be affected by oxygen deprivation and restored by the treatment leading to ROS and oxidative stress reduction. Despite the need for further studies regarding redox modulation in other cellular members of the peri-vascular niche, thus far I-152 demonstrated potent antioxidant properties in a hypoxic environment.

AUTHOR CONTRIBUTIONS

Alessandra Fraternale designed the study, oversaw the execution, and helped in data analyses and interpretation. Michela Bruschi was responsible for establishing the experimentation, data analyses, and interpretation and drafting the manuscript. Francesca Bartoccini synthesized the investigated pro-drug. Michela Bruschi, Federica Biancucci, and Michele Menotta performed metabolomic and proteomic studies. Daniela Ligi and Ferdinando Mannello contributed to cytokine panel analyses. Michela Bruschi, Francesco Piacente, and Santina Bruzzone carried out the fluorescence study. Sofia Masini helped in data collection and interpretation. Mauro Magnani and Antonella Antonelli were responsible for study planning, result discussion, and manuscript revision. All authors read and approved the submission of the manuscript.

CONFLICT OF INTEREST STATEMENT
The authors declare that there is no conflict of interest.

DATA AVAILABILITY STATEMENT
All data generated or analyzed during this study are available upon request to the authors.

ORCID
Michela Bruschi https://orcid.org/0000-0002-0804-7511

REFERENCES
1. Müller N, Warwick T, Noack K, Malacarne PF, Cooper AJL, Weissmann N, et al. Reactive oxygen species differentially modulate the metabolic and transcriptomic response of endothelial cells. Antioxidants. 2022;11(2):434.
2. Bruschi M, Vanzolini T, Sahu N, Balduini A, Magnani M, Fraternale A. Functionalized 3D scaffolds for engineering the hematopoietic niche. Front Bioeng Biotechnol. 2022;10:968086.
3. Bruschi M, Agarwal P, Bhutani N. Induced pluripotent stem cells–derived chondrocyte progenitors. iPSC Derived Progenitors. 2022;13:159–76.
4. Dienemann S, Schmidt V, Fleischhammer T, Mueller JH, Lavrentieva A. Comparative analysis of hypoxic response of human microvascular and umbilical vein endothelial cells in 2D and 3D cell culture systems. J Cell Physiol. 2023;238: 1111–20.
5. Morganti C, Cabezas-Wallscheid N, Ito K. Metabolic regulation of hematopoietic stem cells. HemaSphere. 2022;6(7):e740.

6. Zhang CC, Sadek HA. Hypoxia and metabolic properties of hematopoietic stem cells. Antioxid Redox Signal. 2014;20(12): 1891–901.

7. Mann Z, Sengar M, Verma YK, Rajalingam R, Raghav PK. Hematopoietic stem cell factors: their functional role in self-renewal and clinical aspects. Front Cell Dev Biol. 2022;10:10.

8. Jang Y-Y, Sharkis SJ. A low level of reactive oxygen species selects for primitive hematopoietic stem cells that may reside in the low-oxygenic niche. Blood. 2007;110(8):3056–63.

9. Henry E, Souissi-Sahraoui I, Deynoux M, Lefèvre A, Barroca V, Campalans A, et al. Human hematopoietic stem/progenitor cells display reactive oxygen species-dependent long-term hematopoietic defects after exposure to low doses of ionizing radiations. Haematologica. 2020;105(8):2044–55.

10. Baldea I, Teacoe I, Olteanu DE, Vaida-Voievod C, Clichici A, Sirbu A, et al. Effects of different hypoxia degrees on endothelial cell cultures—time course study. Mech Ageing Dev. 2018; 172:45–50.

11. Cao H, Yu D, Yan X, Wang B, Yu Z, Song Y, et al. Hypoxia destroys the microstructure of microtubules and causes dysfunction of endothelial cells via the PI3K/Stathmin1 pathway. Cell Biosci. 2019;9(1):20.

12. Abaci HE, Truitt R, Luong E, Drazer G, Gerecht S. Adaptation to oxygen deprivation in cultures of human pluripotent stem cells, endothelial progenitor cells, and umbilical vein endothelial cells. Am J Physiol Cell Physiol. 2010;298(6):C1527–37.

13. Li X, Zhang Q, Nasser M, Xu L, Zhang X, Zhu P, et al. Oxygen homeostasis and cardiovascular disease: a role for HIF? Biomed Pharmacother. 2020;128:110338.

14. Samanta D, Semenza GL. Maintenance of redox homeostasis by hypoxia-inducible factors. Redox Biol. 2017;13:331–5.

15. Antonelli A, Scarpa ES, Magnani M. Human red blood cells modulate cytokine expression in monocytes/macrophages under anoxic conditions. Front Physiol. 2021;12:632682.

16. Smith KA, Waypa GB, Schumacker PT. Redox signaling during hypoxia in mammalian cells. Redox Biol. 2017;13:228–34.

17. Bagulho A, Vilas-Boas F, Pena A, Peneda C, Santos FC, Jerónimo A, et al. The extracellular matrix modulates H_2O_2 degradation and redox signaling in endothelial cells. Redox Biol. 2015;6:454–60.

18. Oiry J, Mialocq P, Puy J-Y, Fretier P, Dereuddre-Bosquet N, Dormont D, et al. Synthesis and biological evaluation in human monocyte-derived macrophages of N-(N-acetyl-L-cysteinyl)-S-acetylcysteamine analogues with potent antioxidant and anti-HIV activities. J Med Chem. 2004;47(7):1789–95.

19. Paul BD, Snyder SH. Therapeutic applications of Cysteamine and Cystamine in neurodegenerative and neuropsychiatric diseases. Front Neurol. 2019;10:1315.

20. Wilmer MJ, Kluijtmans LAJ, van der Velden TJ, Willems PH, Scheffer PG, Masereeuw R, et al. Cysteamine restores glutathione redox status in cultured cystinotic proximal tubular epithelial cells. Biochim Biophys Acta. 2011;1812(6):643–51.

21. Atallah C, Charcosset C, Greige-Gerges H. Challenges for cysteamine stabilization, quantification, and biological effects improvement. J Pharm Anal. 2020;10(6):499–516.

22. Schmitt B, Vicenzi M, Garrel C, Denis FM. Effects of N-acetylcysteine, oral glutathione (GSH) and a novel sublingual form of GSH on oxidative stress markers: a comparative crossover study. Redox Biol. 2015;6:198–205.

23. Oiry J, Mialocq P, Puy JY, Fretier P, Clayette P, Dormont D, et al. NAC/MEA conjugate: a new potent antioxidant which increases the GSH level in various cell lines. Bioorg Med Chem Lett. 2001;11(9):1189–91.

24. Brundu S, Palma L, Picceri GG, Ligi D, Orlandi C, Galluzzi L, et al. Glutathione depletion is linked with Th2 polarization in mice with a retrovirus-induced immunodeficiency syndrome, murine AIDS: role of Proglutathione molecules as immunotherapeutics. J Virol. 2016;90(16):7118–30.

25. Crinelli R, Zara C, Galluzzi L, Buffi G, Ceccarini C, Smietana M, et al. Activation of NRF2 and ATF4 signaling by the pro-glutathione molecule I-152, a co-drug of N-acetyl-cysteine and cysteamine. Antioxidants. 2021;10(2):175.

26. Rushworth GF, Megson IL. Existing and potential therapeutic uses for N-acetylcysteine: the need for conversion to intracellular glutathione for antioxidant benefits. Pharmacol Ther. 2014; 141(2):150–9.

27. Xiao W, Loscalzo J. Metabolic responses to reductive stress. Antioxid Redox Signal. 2020;32(18):1330–47.

28. Mansfield KD, Simon MC, Keith B. Hypoxic reduction in cellular glutathione levels requires mitochondrial reactive oxygen species. J Appl Physiol. 2004;97(4):1358–66.

29. Jaganjac M, Milkovic L, Sunjic SB, Zarkovic N. The NRF2, Thioredoxin, and glutathione system in tumorigenesis and anticancer therapies. Antioxidants. 2020;9(11):1151.

30. Tonelli C, Chio IIC, Tuveson DA. Transcriptional regulation by Nrf2. Antioxid Redox Signal. 2018;29(17):1727–45.

31. Chen X, Cao X, Xiao W, Li B, Xue Q. PRDX5 as a novel binding partner in Nrf2-mediated NSCLC progression under oxidative stress. Aging. 2020;12(1):122–37.

32. Bolduc J, Koruza K, Luo T, Malo Pueyo J, Vo TN, Ezeriņa D, et al. Peroxiredoxins wear many hats: factors that fashion their peroxide sensing personalities. Redox Biol. 2021;42:101959.

33. Bartoccini F, Retini M, Crinelli R, Menotta M, Fraternale A, Piersanti G. Dithiol based on l-cysteine and cysteamine as a disulfide-reducing agent. J Org Chem. 2022;87(15):10073–9.

34. Fraternale A, De Angelis M, De Santis R, et al. Targeting SARS-CoV-2 by synthetic dual-acting thiol compounds that inhibit spike/ACE2 interaction and viral protein production. FASEB J. 2023;37(2):e22741.

35. Fraternale A, Zara C, Pierigè F, Rossi L, Ligi D, Amagliani G, et al. Redox homeostasis as a target for new antimycobacterial agents. Int J Antimicrob Agents. 2020;56(4):106148.

36. Petrova B, Warren A, Vital NY, Culhane AJ, Maynard AG, Wong A, et al. Redox metabolism measurement in mammalian cells and tissues by LC-MS. Metabolites. 2021;11(5):313.

37. Motterlini R, Foresti R, Bassi R, Calabrese V, Clark JE, Green CJ. Endothelial heme oxygenase-1 induction by hypoxia. Modulation by inducible nitric-oxide synthase and S-nitrosothiols. J Biol Chem. 2000;275(18):13613–20.

38. Cohen EB, Geck RC, Toker A. Metabolic pathway alterations in microvascular endothelial cells in response to hypoxia. PLoS One. 2020;15(7):e0232072.

39. Fraternale A, Zara C, Di Mambro T, et al. I-152, a supplier of N-acetyl-cysteine and cysteamine, inhibits immunoglobulin secretion and plasma cell maturation in LP-BM5 murine leukemia retrovirus-infected mice by affecting the unfolded protein response. Biochim Biophys Acta Mol Basis Dis. 2020;1866(12): 165922.

40. Wong BW, Marsch E, Treps L, Baes M, Carmeliet P. Endothelial cell metabolism in health and disease: impact of hypoxia. EMBO J. 2017;36(15):2187–203.

41. Xiao W, Wang R-S, Handy DE, Loscalzo J. NAD(H) and NADP(H) redox couples and cellular energy metabolism. Antioxid Redox Signal. 2018;28(3):251–72.

42. Sorgdrager FJH, Naudé PJW, Kema IP, Nollen EA, Deyn PPD. Tryptophan metabolism in Inflammaging: from biomarker to therapeutic target. Front Immunol. 2019;10:10.

43. Engl E, Garvert MM. A prophylactic role for creatine in hypoxia? J Neurosci. 2015;35(25):9249–51.

44. Clarke H, Hickner RC, Ormsbee MJ. The potential role of creatine in vascular health. Nutrients. 2021;13(3):857.

45. Arazi H, Eghbali E, Suzuki K. Creatine supplementation, physical exercise and oxidative stress markers: a review of the mechanisms and effectiveness. Nutrients. 2021;13(3):869.

46. Wu X, Zhang L, Miao Y, Yang J, Wang X, Wang CC, et al. Homocysteine causes vascular endothelial dysfunction by disrupting endoplasmic reticulum redox homeostasis. Redox Biol. 2019;20:46–59.

47. Antonelli A, Scarpa ES, Bruzzone S, Astigiano C, Piacente F, Bruschi M, et al. Anoxia rapidly induces changes in expression of a large and diverse set of genes in endothelial cells. Int J Mol Sci. 2023;24(6):5157.

48. Bartoszewski R, Moszyńska A, Serocki M, Cabaj A, Polten A, Ochocka R, et al. Primary endothelial cell-specific regulation of hypoxia-inducible factor (HIF)-1 and HIF-2 and their target gene expression profiles during hypoxia. FASEB J. 2019;33(7): 7929–41.

49. Hashimoto T, Shibasaki F. Hypoxia-inducible factor as an angiogenic master switch. Front Pediatr. 2015;3:3.

50. Hansen JM, Zhang H, Jones DP. Differential oxidation of thioredoxin-1, thioredoxin-2, and glutathione by metal ions*. Free Radic Biol Med. 2006;40(1):138–45.

51. Hasan AA, Kalinina E, Tatarskiy V, Shtil A. The thioredoxin system of mammalian cells and its modulators. Biomedicine. 2022;10(7):1757.

52. Kandarakov O, Belyavsky A, Semenova E. Bone marrow niches of hematopoietic stem and progenitor cells. Int J Mol Sci. 2022; 23(8):4462.

53. King KY, Goodell MA. Inflammatory modulation of hematopoietic stem cells: viewing the hematopoietic stem cell as a foundation for the immune response. Nat Rev Immunol. 2011; 11(10):685–92.

54. Kikuchi A, Pradhan-Sundd T, Singh S, Nagarajan S, Loizos N, Monga SP. Platelet-derived growth factor receptor α contributes to human hepatic stellate cell proliferation and migration. Am J Pathol. 2017;187(10):2273–87.

55. Babicki S, Arndt D, Marcu A, Liang Y, Grant JR, Maciejewski A, et al. Heatmapper: web-enabled heat mapping for all. Nucleic Acids Res. 2016;44(W1):W147–53.

56. Szklarczyk D, Gable AL, Nastou KC, Lyon D, Kirsch R, Pyysalo S, et al. The STRING database in 2021: customizable protein-protein networks, and functional characterization of user-uploaded gene/measurement sets. Nucleic Acids Res. 2021;49(D1):D605–12.

57. Jensen LJ, Kuhn M, Stark M, Chaffron S, Creevey C, Muller J, et al. STRING 8—a global view on proteins and their functional interactions in 630 organisms. Nucleic Acids Res. 2009;37(Database issue):D412–6.

58. Aoyama K, Nakaki T. Inhibition of GTRAP3-18 may increase neuroprotective glutathione (GSH) synthesis. Int J Mol Sci. 2012;13(9):12017–35.

59. Lu SC. Regulation of hepatic glutathione synthesis: current concepts and controversies. FASEB J. 1999;13(10):1169–83.

60. Ji Y, Bennett BM. Activation of microsomal glutathione S-transferase by peroxynitrite. Mol Pharmacol. 2003;63(1): 136–46.

61. Munro D, Banh S, Sotiri E, Tamanna N, Treberg JR. The thioredoxin and glutathione-dependent H_2O_2 consumption pathways in muscle mitochondria: involvement in H_2O_2 metabolism and consequence to H_2O_2 efflux assays. Free Radic Biol Med. 2016;96:334–46.

62. Congrains A, Bianco J, Rosa RG, Mancuso RI, Saad STO. 3D scaffolds to model the hematopoietic stem cell niche: applications and perspectives. Materials. 2021;14(3):569.

63. Nombela-Arrieta C, Silberstein LE. The science behind the hypoxic niche of hematopoietic stem and progenitors. Hematology. 2014;2014(1):542–7.

64. Bruschi M, Sahu N, Singla M, Grandi F, Agarwal P, Chu C, et al. A quick and efficient method for the generation of immunomodulatory mesenchymal stromal cell from human induced pluripotent stem cell. Tissue Eng Part A. 2021;28:433–46.

65. Wilkinson AC, Nakauchi H. Stabilizing hematopoietic stem cells in vitro. Curr Opin Genet Dev. 2020;64:1–5.

66. Wang X, Cooper S, Broxmeyer HE, Kapur R. Nuclear translocation of TFE3 under hypoxia enhances the engraftment of human hematopoietic stem cells. Leukemia. 2022;36(8):2144–8.

67. Bozhilov YK, Hsu I, Brown EJ, Wilkinson AC. In vitro human Haematopoietic stem cell expansion and differentiation. Cell. 2023;12(6):896.

68. Hadland B, Varnum-Finney B, Dozono S, Dignum T, Nourigat-McKay C, Heck AM, et al. Engineering a niche supporting hematopoietic stem cell development using integrated single-cell transcriptomics. Nat Commun. 2022;13(1):1584.

69. Warpsinski G, Smith MJ, Srivastava S, Keeley TP, Siow RCM, Fraser PA, et al. Nrf2-regulated redox signaling in brain endothelial cells adapted to physiological oxygen levels: consequences for sulforaphane mediated protection against hypoxia-reoxygenation. Redox Biol. 2020;37:101708.

70. Yang C, Zhang X, Ge X, He C, Liu S, Yang S, et al. N-Acetylcysteine protects against cobalt chloride-induced endothelial dysfunction by enhancing glucose-6-phosphate dehydrogenase activity. FEBS Open Bio. 2022;12(8):1475–88.

71. Krause BJ, Casanello P, Dias AC, Arias P, Velarde V, Arenas GA, et al. Chronic intermittent hypoxia-induced vascular dysfunction in rats is reverted by N-Acetylcysteine supplementation and arginase inhibition. Front Physiol. 2018;9:901.

72. Khomenko T, Deng X, Sandor Z, Tarnawski AS, Szabo S. Cysteamine alters redox state, HIF-1α transcriptional interactions and reduces duodenal mucosal oxygenation: novel insight into the mechanisms of duodenal ulceration. Biochem Biophys Res Commun. 2004;317(1):121–7.

73. Shin YJ, Seo JM, Chung TY, Hyon JY, Wee WR. Effect of cysteamine on oxidative stress-induced cell death of human corneal endothelial cells. Curr Eye Res. 2011;36(10):910–7.

74. Samuni Y, Goldstein S, Dean OM, Berk M. The chemistry and biological activities of N-acetylcysteine. Biochim Biophys Acta. 2013;1830(8):4117–29.

75. Martín-Sabroso C, Alonso-González M, Fernández-Carballido A, Aparicio-Blanco J, Córdoba-Díaz D, Navarro-García F, et al. Limitations and challenges in the stability of cysteamine eye drop compounded formulations. Pharmaceuticals. 2021;15(1):2.

76. Ezeriņa D, Takano Y, Hanaoka K, Urano Y, Dick TP. N-acetyl cysteine functions as a fast-acting antioxidant by triggering intracellular H_2S and sulfane sulfur production. Cell Chem Biol. 2018;25(4):447–459.e4.

77. Dai X, Wang K, Fan J, Liu H, Fan X, Lin Q, et al. Nrf2 transcriptional upregulation of IDH2 to tune mitochondrial dynamics and rescue angiogenic function of diabetic EPCs. Redox Biol. 2022;56:102449.

78. Cano M, Datta S, Wang L, Liu T, Flores-Bellver M, Sachdeva M, et al. Nrf2 deficiency decreases NADPH from impaired IDH shuttle and pentose phosphate pathway in retinal pigmented epithelial cells to magnify oxidative stress-induced mitochondrial dysfunction. Aging Cell. 2021;20(8):e13444.

79. Le Gal K, Schmidt EE, Sayin VI. Cellular redox homeostasis. Antioxidants. 2021;10(9):1377.

80. Tanaka LY, Oliveira PVS, Laurindo FRM. Peri/epicellular thiol oxidoreductases as mediators of extracellular redox signaling. Antioxid Redox Signal. 2020;33(4):280–307.

81. Kocabas F, Xie L, Xie J, Yu Z, DeBerardinis RJ, Kimura W, et al. Hypoxic metabolism in human hematopoietic stem cells. Cell Biosci. 2015;5(1):39.

82. Tajima M, Kurashima Y, Sugiyama K, Ogura T, Sakagami H. The redox state of glutathione regulates the hypoxic induction of HIF-1. Eur J Pharmacol. 2009;606(1):45–9.

83. Gerber H-P, Ferrara N. The role of VEGF in normal and neoplastic hematopoiesis. J Mol Med (Berl). 2003;81(1):20–31.

84. Cohen T, Nahari D, Cerem LW, Neufeld G, Levi B-Z. Interleukin 6 induces the expression of vascular endothelial growth factor (*). J Biol Chem. 1996;271(2):736–41.

85. Fu X, Zhai S, Yuan J. Interleukin-6 (IL-6) triggers the malignancy of hemangioma cells via activation of HIF-1α/VEGFA signals. Eur J Pharmacol. 2018;841:82–9.

86. Pearlstein DP, Ali MH, Mungai PT, Hynes KL, Gewertz BL, Schumacker PT. Role of mitochondrial oxidant generation in endothelial cell responses to hypoxia. Arterioscler Thromb Vasc Biol. 2002;22(4):566–73.

87. Ali MH, Schlidt SA, Chandel NS, Hynes KL, Schumacker PT, Gewertz BL. Endothelial permeability and IL-6 production during hypoxia: role of ROS in signal transduction. Am J Physiol. 1999;277(5):L1057–65.

88. Tarbell J, Mahmoud M, Corti A, Cardoso L, Caro C. The role of oxygen transport in atherosclerosis and vascular disease. J R Soc Interface. 2020;17(165):20190732.

SUPPORTING INFORMATION

Additional supporting information can be found online in the Supporting Information section at the end of this article.

How to cite this article: Bruschi M, Biancucci F, Masini S, Piacente F, Ligi D, Bartoccini F, et al. The influence of redox modulation on hypoxic endothelial cell metabolic and proteomic profiles through a small thiol-based compound tuning glutathione and thioredoxin systems. BioFactors. 2023. https://doi.org/10.1002/biof.1988